

Kinetics of the Gas-Phase Reactions of OH and NO₃ Radicals with Dimethylphenols

Lars P. Thüner, Perla Bardini, Gerard J. Rea, and John C. Wenger*

Department of Chemistry and Environmental Research Institute, University College Cork, Cork, Ireland

Received: August 12, 2004; In Final Form: September 29, 2004

Rate coefficients for the reactions of hydroxyl (OH) and nitrate (NO₃) radicals with the six dimethylphenols have been determined at 295 ± 2 K and atmospheric pressure using the relative rate technique. Experiments were performed in a 3.91 m³ atmospheric simulation chamber using in situ FTIR spectroscopy and gas chromatography for chemical analysis. The reactivity of the dimethylphenols is compared to other phenolic compounds and it is shown that the rate coefficients strongly depend on the number and position of the OH and CH₃ substituents around the aromatic ring. In addition, the dimethylphenol isomers appear to exhibit an opposite trend in reactivity for reaction with OH and NO₃ radicals. The rate coefficient data for the dimethylphenols and related phenolic compounds are explained in terms of known mechanistic features of the reactions. The atmospheric implications are also discussed.

Introduction

Aromatic compounds, such as benzene, toluene and the xylenes, are one of the most important classes of primary pollutants. They are emitted into the atmosphere from solvents, fuels, and vehicle exhaust gases and in total, account for around 10% of the total global nonmethane hydrocarbon emissions.¹ The high reactivity of aromatics with hydroxyl (OH) radicals in the atmosphere means that they also contribute greatly to the formation of secondary pollutants such as ozone and nitrates, which are major constituents of photochemical smog. Indeed, it has been estimated that their contribution to ozone production in the U.K. could be as high as 30%.²

The OH radical initiated oxidation of benzene, toluene, and the xylenes produces phenol, cresols, and dimethylphenols respectively.³ To fully understand the environmental impact of aromatic compounds, a detailed knowledge of the atmospheric degradation processes for these reaction products is also required. The major atmospheric loss processes for phenolic compounds are gas-phase reaction with hydroxyl and nitrate (NO₃) radicals.⁴ The relative contribution of these reactions to the atmospheric loss of the phenols is dependent on the magnitude of the rate coefficients for the reactions and the ambient concentrations of the radical species. To date, laboratory kinetic studies have largely focused on the phenols and cresols. Rate coefficients for the reactions of these compounds with OH^{5–10} and NO₃^{11–14} have been reported on several occasions. However, the reactions of the dimethylphenols with OH have only been studied once before¹⁰ and no data concerning their reaction with NO₃ are available.

The aim of this work was to determine rate coefficients for the reaction of the dimethylphenols with OH and NO₃ radicals to assess the relative importance of these reactions as atmospheric loss processes. The reactivity of the dimethylphenols is compared to other phenolic compounds, and several interesting reactivity patterns emerge. These observations are interpreted in light of the current understanding of the atmospheric chemistry of aromatic compounds.

Experimental Section

Experiments were performed in a newly constructed atmospheric simulation chamber equipped with gas chromatography and in situ FTIR spectroscopy for chemical analysis.¹⁵ The chamber has a cylindrical shape and consists of a FEP (fluorine-ethene-propene) foil tube (4.1 m long, 1.1 m diameter and 0.127 mm thickness, supplied by Foiltec, Bremen, Germany) closed at both ends by FEP foil covered aluminum plates (15 mm thickness). At atmospheric pressure the chamber has a volume of 3.91 m³ and a volume to surface area ratio of ca. 0.24 m. The ends of the tube have O-rings sealed into the foil that enable it to be clamped onto the end plates using circular aluminum segments, thus ensuring that the chamber is leak-tight. The chamber is surrounded by 18 Philips TUV (40 W) lamps with an emission maximum at 254 nm and 18 Philips TL05 (40 W) lamps with an emission maximum at 360 nm. The lamps are wired in parallel and can be switched individually to allow control of light intensity and wavelength. The end plates, cylindrical foil, and lamps are supported by a frame constructed of aluminum profiles (60 mm thickness, Bosch) and covered with aluminum sheets to prevent light from escaping. Both end plates are fitted with five symmetrically positioned removable flanges. The large central flanges are used to support the field and objective mirrors required for long path in situ FTIR spectroscopy, whereas the others are used for the introduction and sampling of gases and for flushing the chamber with air.

The optical arrangement for in situ FTIR spectroscopy was designed in conjunction with Dr. Klaus Brockmann of the Bergische Universität Wuppertal. It consists of a White cell with two circular field mirrors (diameter 254 mm) and a rectangular objective mirror (200 mm × 406 mm) separated by 3.82 ± 0.01 m. The mirrors, manufactured by Lichtenknecker Optics, are made of Pyrex, gold-coated, and mounted on adjustable screws to facilitate alignment of the optical system. The infrared spectrometer (BioRad Excalibur) is interfaced to the chamber via a transfer optics arrangement consisting of 12 gold-coated mirrors (Bernard Halle Optics). The infrared beam enters and leaves the chamber through KBr windows (50 mm diameter, 3 mm thickness, Moltech, Berlin) and passes through two cut-out edges in the objective mirror. The White system was

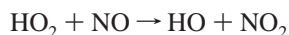
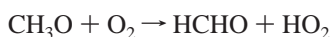
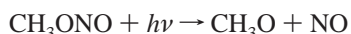
* To whom correspondence should be addressed. Tel: +353 21 4902454. Fax: +353 21 4903014. E-mail: j.wenger@ucc.ie.

operated at 60 traverses; this path length combined with twice the distance from the surface of the objective mirror to the wall of the chamber, gives a total optical path length of 229.6 ± 0.6 m.

The chamber is operated using purified dry air at 0.1–1 mbar above atmospheric pressure, as monitored by a differential pressure transducer (MKS instruments) located on one of the end-plate flanges. The purified air is generated by an air purification system (Zander KMA 75) that runs on compressed air and reduces concentrations of NO_x and nonmethane hydrocarbons to $< 2.5 \times 10^{11}$ molecules cm^{-3} . The temperature and amount of water vapor in the chamber is monitored by a dewpoint meter (Vaisala DM70). Experiments are performed at 295 ± 2 K and at a dewpoint temperature of 223 ± 5 K. Between experiments the chamber is cleaned by flushing with the purified air at a flow rate of $0.15 \text{ m}^3 \text{ min}^{-1}$ for a minimum of 4 h.

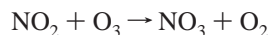
Rate coefficients for the reactions of the dimethylphenols with OH and NO_3 were determined using a relative rate method in which the decay rates of the compounds were measured relative to that of a reference organic compound. Experiments were performed on the six dimethylphenols individually using 1,3,5-trimethylbenzene and *o*-cresol as the reference compounds for reactions with OH and NO_3 , respectively. The dimethylphenols and reference compounds were introduced into the reaction chamber using an inlet system in which weighed amounts of the substances were heated in a flow of purified air. The inlet lines were also heated to avoid condensation of the semivolatile compounds before entering the chamber. At the start of each experiment, the organic compounds were left in the chamber for at least 2 h and often overnight to determine their rate of deposition to the walls of the reactor. These loss rates were used to quantify the contribution of surface deposition to the measured overall decay of the compounds during the experiments.

The hydroxyl radical reactions were performed using the photolysis of methyl nitrite (by the Philips TL05 lamps) as the radical source:



Measured amounts of methyl nitrite were flushed from a calibrated Pyrex bulb into the chamber by a stream of purified air. The initial reactant concentrations (in molecule cm^{-3}) were as follows: $[\text{CH}_3\text{ONO}] = (1.2\text{--}2.0) \times 10^{14}$, $[\text{dimethylphenol}] = (2.5\text{--}5.0) \times 10^{13}$, and $[1,3,5\text{-trimethylbenzene}] = (2.5\text{--}3.8) \times 10^{13}$. The reactant mixtures were photolyzed for 1 min, and an infrared spectrum of the chamber contents was recorded. This photolysis-sampling procedure was repeated 6–8 times until around 30% depletion of the reference and substrate compounds was achieved. Infrared spectra were obtained at a resolution of 1 cm^{-1} using a narrow-band MCT detector and derived from the co-addition of 250 scans collected over 5 min. Quantitative analysis was performed by linear subtraction of calibrated reference spectra of known compounds and subsequent integration of selected absorption bands for the dimethylphenols and reference compound. At least three experiments were carried out with each of the dimethylphenols.

The nitrate radical reactions were performed using the reaction of NO_2 and O_3 as the radical source:



The reactant gases were flowed through an S-shaped Pyrex tube and into the chamber containing the reactant and reference compounds. The flow rates of the gases were adjusted to ensure that an excess of NO_2 was present. Under these conditions, the NO_2 can also react with nitrate radicals to form N_2O_5 , which acts a temporary reservoir of NO_3 through the following equilibrium:



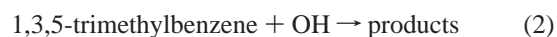
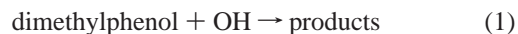
A number of precautions were taken to eliminate the possibility of competing reactions occurring. First, the substrate and reference compounds were allowed to mix in the chamber with NO_2 for several hours while the concentrations of the hydrocarbons were monitored. No reaction was observed, thus confirming that reaction with NO_2 was negligible. Second, because the cresols (and possibly the dimethylphenols) are known to react slowly with ozone, e.g., $k_{\text{O}_3} = 3 \times 10^{-19} \text{ cm}^3 \text{ molecule}^{-1} \text{ s}^{-1}$ for *o*-cresol,³ the flow rates of the gases were adjusted to ensure that NO_2 was in sufficient excess to react with all of the ozone in the flow tube before reaching the chamber. The amount of ozone entering the chamber was always less than the detection limits provided by FTIR spectroscopy (ca. $0.5 \times 10^{13} \text{ molecule cm}^{-3}$).

The initial reactant concentrations (in molecule cm^{-3}) were as follows: $[\text{dimethylphenol}] = (1.25\text{--}3.75) \times 10^{14}$ and $[\textit{o}\text{-cresol}] = (1.25\text{--}3.75) \times 10^{14}$. During each experiment, successive additions of NO_2 [$(1.5\text{--}4.5) \times 10^{13} \text{ molecule cm}^{-3}$] and O_3 [$(0.5\text{--}1.5) \times 10^{13} \text{ molecule cm}^{-3}$] were performed. The concentrations of the reactant and reference compounds were monitored by gas chromatography. The gas chromatograph (Varian 3800), equipped with flame ionization detection, is connected to the reactor via a 6 port gas sampling valve (Valco). The valve is fitted with a 1 cm^3 sampling loop and is equipped with a pneumatically controlled actuator to enable automated injection of reaction mixtures onto the column. Chromatographic separation was achieved by using a 30 m WCOT infused silica capillary column (CP-Sil 8CB) operated at 423 K. Sampling was carried out 12 min after the addition of NO_3 radicals and at further 12 min intervals. When the concentration of the organic compounds stabilized, thus indicating that the reaction was complete, another addition of NO_2 and O_3 was performed. Typically, 8–10 additions were made in each experiment. Relative concentrations of substrate and reference compounds were determined from peak area measurements during analyses. At least three experiments were carried out with each of the dimethylphenols.

All dimethylphenols and reference compounds used in this study were obtained from Aldrich Chemical Co. (stated purities $> 98\%$) and used without further purification. Methyl nitrite was synthesized following the method of Taylor et al.¹⁶ and its purity checked by FTIR spectroscopy. Nitrogen dioxide ($> 98\%$) was obtained from BOC gases. Ozone was generated by passing oxygen through an ozone generator (Yanco GE60/FM5000).

Results

Rate coefficients for the reactions of the dimethylphenols (DMPs) with OH were determined by comparing the rates of decay of the reactant relative to that of the reference compound 1,3,5-trimethylbenzene (1,3,5-TMB):



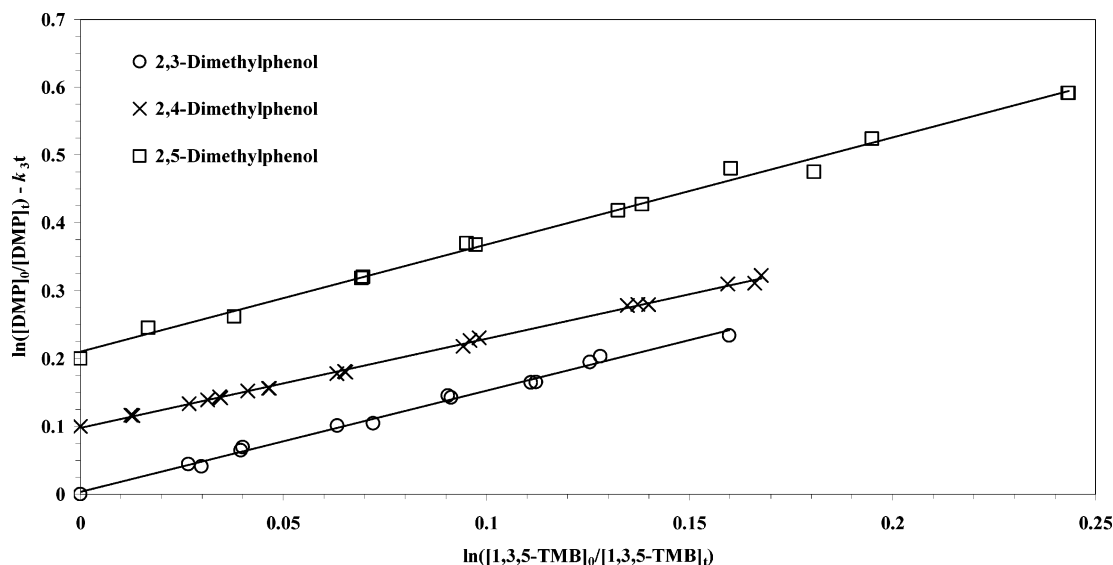
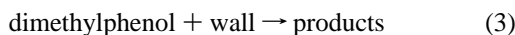


Figure 1. Relative rate plots for the reaction of OH radicals with 2,3-, 2,4-, and 2,5-dimethylphenol at 295 ± 2 K. For reasons of clarity, the data for 2,4- and 2,5-dimethylphenol have been displaced vertically by 0.1 and 0.2 units, respectively.

The dimethylphenols were also lost to the walls of the reactor via deposition:

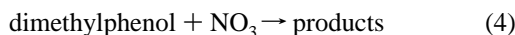


There was no observed wall deposition for 1,3,5-trimethylbenzene. Integrating and combining eqs 1–3 yields the following relationship:

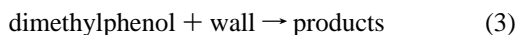
$$\ln \frac{[\text{DMP}]_0}{[\text{DMP}]_t} - k_3 t = \frac{k_1}{k_2} \ln \frac{[1,3,5\text{-TMB}]_0}{[1,3,5\text{-TMB}]_t} \quad (I)$$

where k_1 , k_2 , and k_3 are the rate coefficients for reactions 1–3 and the subscripts 0 and t indicate concentrations at the start of the reaction and at time t , respectively.

Rate coefficients for the reactions of the dimethylphenols with NO₃ were determined by comparing the rates of decay of the reactant relative to that of the reference compound *o*-cresol:



The dimethylphenols and *o*-cresol were also lost to the walls of the reactor via deposition:



Integrating and combining eqs 3–6 yields the following relationship:

$$\ln \frac{[\text{DMP}]_0}{[\text{DMP}]_t} - k_3 t = \frac{k_4}{k_5} \ln \frac{[o\text{-cresol}]_0}{[o\text{-cresol}]_t} - k_6 t \quad (II)$$

where k_4 , k_5 , and k_6 are the rate coefficients for reactions 4–6 and the subscripts 0 and t indicate concentrations at the start of the reaction and at time t , respectively.

The concentrations of reactant and reference compounds were determined directly by FTIR spectroscopy during OH reactions and gas chromatography during NO₃ reactions. The rates of loss of the dimethylphenols and *o*-cresol to the walls of the chamber were determined by measuring the decay of the compounds over

a period of at least 2 h prior to the start of every experiment. Values of $k_3 = (2.0\text{--}8.6) \times 10^{-6} \text{ s}^{-1}$ and $k_6 = (4.6\text{--}6.1) \times 10^{-6} \text{ s}^{-1}$ were obtained for the dimethylphenols and *o*-cresol, respectively. The wall loss rates were found to vary by up to 30% in some cases, indicating that the wall loss rate was probably influenced by the cleanliness of the chamber surfaces. As a result, the values of k_3 and k_6 were determined prior to the start of each experiment. Wall loss accounted for 3–9% of the overall decay of the dimethylphenol compounds in the OH experiments. During the NO₃ experiments wall loss was responsible for 3–11% of the decay of the dimethylphenols and 4–8% of *o*-cresol.

Data generated from the OH reactions were plotted in the form of eq I and are shown in Figures 1 and 2. Data generated from the NO₃ reactions were plotted in the form of eq II and are shown in Figures 3 and 4. The plots show good linearity and have near-zero intercepts. Rate coefficients for the reaction of OH radicals with the dimethylphenols (k_1) were calculated from the gradients of the plots (k_1/k_2) using a value of $k_2 = (5.59 \pm 0.48) \times 10^{-11} \text{ cm}^3 \text{ molecule}^{-1} \text{ s}^{-1}$.¹⁷ Similarly, rate coefficients for the reaction of NO₃ radicals with the dimethylphenols (k_4) were calculated from the gradients of the plots (k_4/k_5) using a value of $k_5 = (1.37 \pm 0.09) \times 10^{-11} \text{ cm}^3 \text{ molecule}^{-1} \text{ s}^{-1}$.¹³ A summary of the rate coefficients is given in Table 1 along with previously reported results. The indicated errors are twice the standard deviation arising from the least-squares fit of the data and only reflect the precision in the measurements, which is $\pm 0.5\text{--}1.0\%$ for gas chromatography and $\pm 5\%$ for FTIR spectroscopy. The quoted uncertainty in the rate coefficient for the reference compound is also incorporated into the indicated errors.

Discussion

Comparison with Previous Studies. The rate coefficients obtained in this study for the reactions of OH radicals with the dimethylphenols are in excellent agreement with those determined by Atkinson and Aschmann,¹⁰ Table 1. The value of $k_{\text{OH}} = (8.17 \pm 0.85) \times 10^{-11} \text{ cm}^3 \text{ molecule}^{-1} \text{ s}^{-1}$ for 2,5-dimethylphenol measured by Volkammer et al.²⁰ using the relative rate technique with 1,3,5-trimethylbenzene as the reference compound is also in good agreement. It is of interest to note that the uncertainties in the rate coefficients reported in

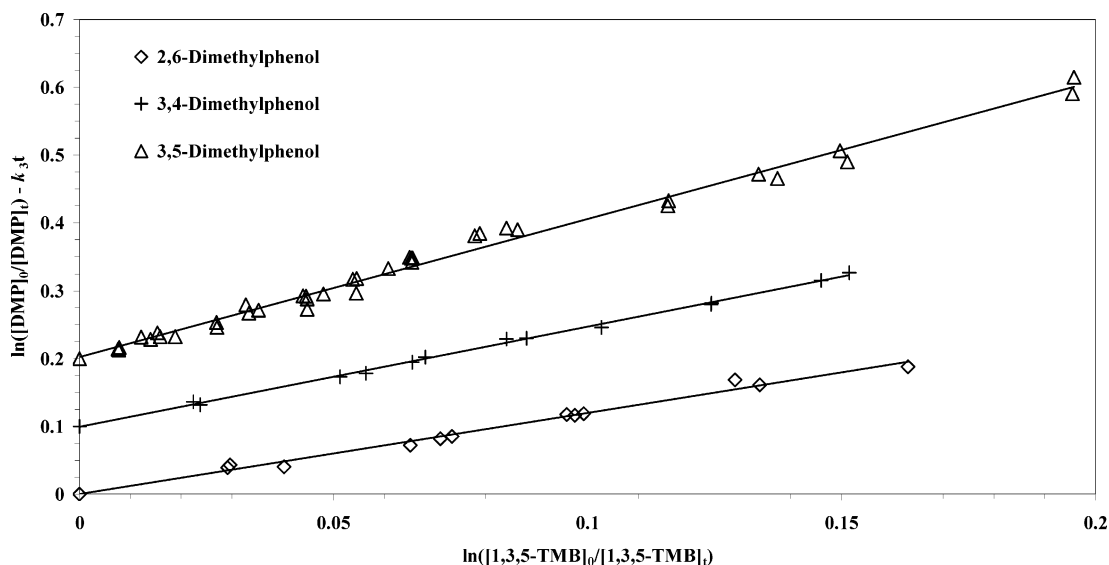


Figure 2. Relative rate plots for the reaction of OH radicals with 2,6-, 3,4-, and 3,5-dimethylphenol at 295 ± 2 K. For reasons of clarity, the data for 3,4- and 3,5-dimethylphenol have been displaced vertically by 0.1 and 0.2 units, respectively.

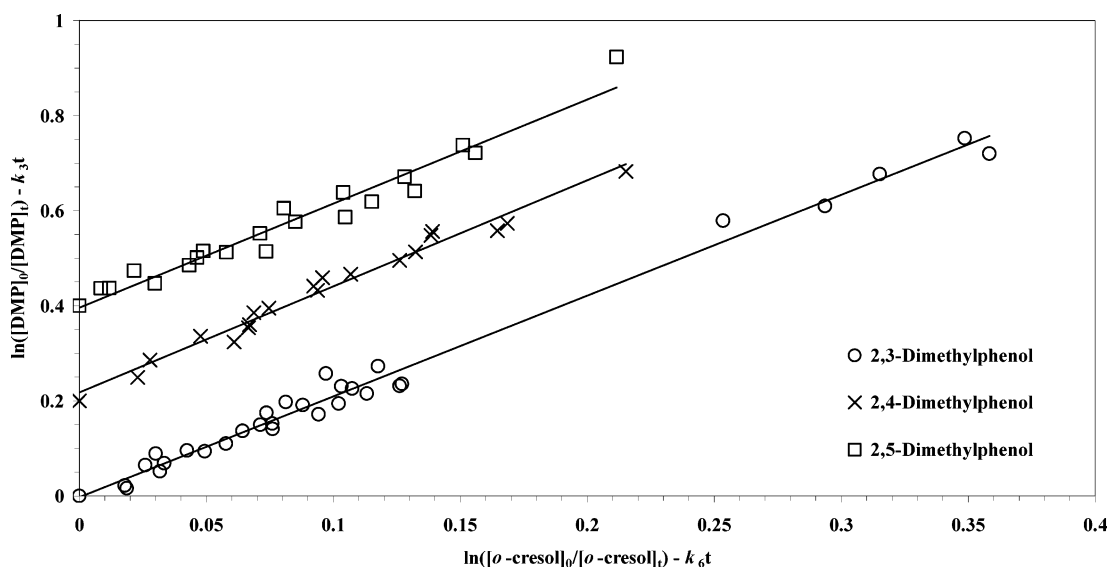


Figure 3. Relative rate plots for the reaction of NO_3 radicals with 2,3-, 2,4-, and 2,5-dimethylphenol at 295 ± 2 K. For reasons of clarity, the data for 2,4- and 2,5-dimethylphenol have been displaced vertically by 0.2 and 0.4 units, respectively.

this work and also that of Volkammer et al. are significantly lower than those reported by Atkinson and Aschmann. A likely explanation for this observation is that the in situ analysis performed in the present study and in the work of Volkammer et al. resulted in lower measurement errors for the dimethylphenols and reference compounds than in the work of Atkinson and Aschmann, who used thermal desorption gas chromatography.¹⁰

This is the first reported study of the reactions of NO_3 radicals with the dimethylphenols, and a comparison with previous work is not possible. However, the rate coefficients determined in this work are the same order of magnitude as those for the cresols and thus are in line with expectations.³

Trends in the Rate Coefficients. In an attempt to rationalize the experimental results for the dimethylphenols, it is useful to compare their reactivity with other phenolic compounds. As shown in Table 2, the dimethylphenols exhibit greater reactivity toward OH and NO_3 radicals than the cresols but are less reactive than the trimethylphenols and 1,2-dihydroxymethylbenzenes. In addition, the cresol and dimethylphenol isomers appear to exhibit opposite trends in reactivity for reaction with

OH and NO_3 , e.g., 3,5 dimethylphenol is the most reactive isomer toward OH but the least reactive toward NO_3 . Clearly the number and positions of the OH or CH_3 substituents has a profound affect on the reactivity of aromatic compounds with OH and NO_3 radicals. However, to date, no detailed interpretation of the rate coefficients has been offered in the literature. The following discussion is an attempt to explain the observed reactivity patterns using the current level of understanding of the reactions of phenolic compounds with OH and NO_3 radicals.³

The reaction of phenolic compounds with OH radicals proceeds predominantly via electrophilic addition of OH to the aromatic ring.⁴ For phenol, only about 9% of the overall reaction is thought to occur via H-atom abstraction from the OH group and for *o*-cresol, about 7% of the reaction is attributed to H-atom abstraction from the OH and CH_3 groups.⁴ Indeed, Olariu et al.²⁴ have shown that for phenol and the cresols, OH addition at the position ortho to the OH substituent dominates, resulting in the formation of dihydroxybenzenes with yields of up to 80%. Thus, it is expected that addition of OH to the aromatic ring also accounts for most of the reactivity of the dimethylphenols. Because electrophilic addition is the major reaction mechanism,

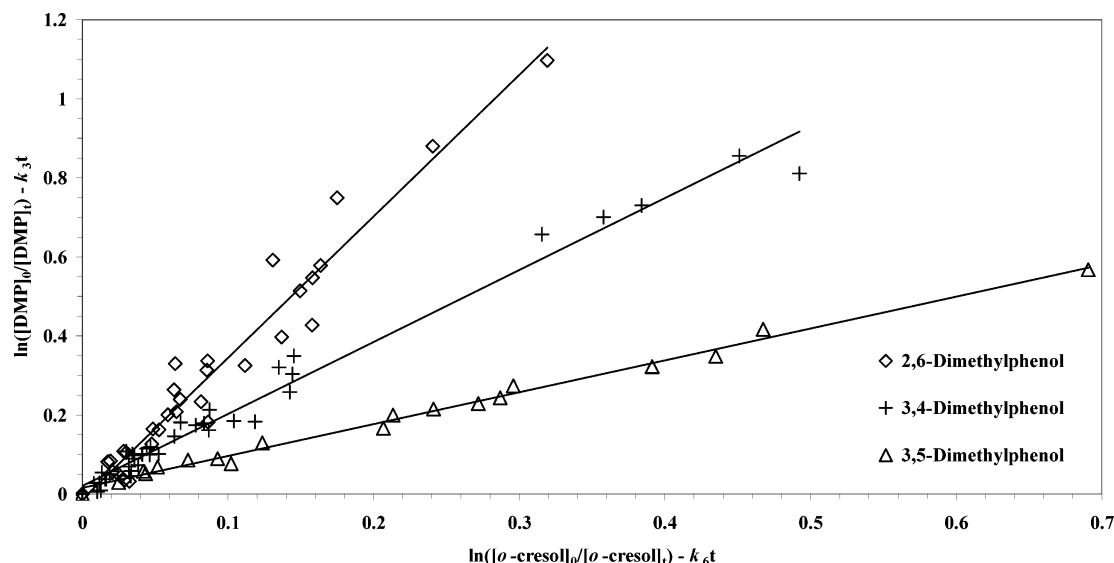


Figure 4. Relative rate plots for the reaction of NO₃ radicals with 2,6-, 3,4-, and 3,5-dimethylphenol at 295 ± 2 K.

TABLE 1: Rate Coefficients for the Reactions of OH and NO₃ Radicals with the Dimethylphenols at 295 ± 2 K and the Associated Atmospheric Lifetimes

compound	k_1/k_2^a	k_4/k_5^a	k_{OH}^b		$k_{NO_3}^b$	τ_{OH}^c (s)	$\tau_{NO_3}^d$ (s)
			this work	literature ¹⁰			
2,3-dimethylphenol	1.49 ± 0.07	2.12 ± 0.04	8.33 ± 1.11	8.02 ± 2.03	2.90 ± 0.25	7502	69
2,4-dimethylphenol	1.32 ± 0.02	2.23 ± 0.08	7.38 ± 0.75	7.15 ± 1.84	3.06 ± 0.31	8468	65
2,5-dimethylphenol	1.58 ± 0.07	2.19 ± 0.11	8.83 ± 1.15	8.00 ± 2.29	3.00 ± 0.35	7078	67
2,6-dimethylphenol	1.19 ± 0.06	3.58 ± 0.16	6.65 ± 0.91	6.59 ± 1.73	4.90 ± 0.54	8635	41
3,4-dimethylphenol	1.48 ± 0.04	1.82 ± 0.04	8.27 ± 0.93	8.14 ± 2.12	2.49 ± 0.22	7558	80
3,5-dimethylphenol	2.04 ± 0.07	0.81 ± 0.02	11.4 ± 1.37	11.3 ± 3.00	1.11 ± 0.10	5482	180

^a Errors are twice the standard deviation arising from the linear regression analysis and represent precision only. ^b In units of 10⁻¹¹ cm³ molecule⁻¹ s⁻¹. ^c $\tau_{OH} = 1/k_{OH}[OH]$, where 12 h daily average [OH] = 1.6 × 10⁶ molecule cm⁻³.¹⁸ ^d $\tau_{NO_3} = 1/k_{NO_3}[NO_3]$, where 12 h daily average [NO₃] = 5 × 10⁸ molecule cm⁻³.¹⁹

TABLE 2: Comparison of the Rate Coefficients for the Reactions of OH and NO₃ Radicals with Dimethylphenols and Selected Other Phenolic Compounds

compound	k_{OH}^a	$k_{NO_3}^a$
phenol	2.7 ^b	0.4 ^b
<i>o</i> -cresol	4.1	1.4
<i>m</i> -cresol	6.8	1.1
<i>p</i> -cresol	5.0	1.1
2,3-dimethylphenol	8.3 ^c	2.9 ^c
2,4-dimethylphenol	7.4	3.1
2,5-dimethylphenol	8.8	3.0
2,6-dimethylphenol	6.7	4.9
3,4-dimethylphenol	8.3	2.5
3,5-dimethylphenol	11.4	1.1
2,3,5-trimethylphenol	12.5 ^d	-
2,3,6-trimethylphenol	11.8 ^d	-
1,2-dihydroxybenzene	10.4 ^e	9.8 ^e
1,2-dihydroxy-3-methylbenzene	20.5	17.1
1,2-dihydroxy-4-methylbenzene	15.6	14.7

^a In units of 10⁻¹¹ cm³ molecule⁻¹ s⁻¹. ^b Rate coefficients for phenol and the cresols are from Calvert et al.³ ^c Rate coefficients for the dimethylphenols are from this work. ^d Rate coefficients for the trimethylphenols are from Tse et al.²¹ ^e Rate coefficients for the dihydroxybenzene compounds are taken from Olariu et al.^{22,23}

the number and position of the OH and CH₃ substituents will have a significant influence on reactivity. The methyl and hydroxyl groups both donate electron density to the aromatic ring and activate the ortho and para positions toward electrophilic addition. This results in the general observation that the reactivity of aromatic compounds toward OH radicals increases with the number of substituent hydroxyl or methyl groups. For example, the order of reactivity in the methyl-substituted

benzenes is trimethylbenzene > dimethylbenzene (xylene) > toluene > benzene³ and in the methyl-substituted phenols is trimethylphenol > dimethylphenol > methylphenol (cresol) > phenol. Similarly, the methyl-substituted 1,2-dihydroxybenzenes are more reactive than 1,2-dihydroxybenzene, which, in turn, is more reactive than phenol.

For compounds with the same number of OH or CH₃ substituents, the relative electron donating strengths of the OH and CH₃ groups are important in determining reactivity. The methyl group acts inductively whereas the hydroxyl group donates electron density via resonance effects. The latter process is more efficient and the aromatic ring is activated to a much greater extent by OH groups than by CH₃ groups. This is clearly illustrated by the following examples; phenol ($k_{OH} = 2.7 \times 10^{-11}$ cm³ molecule⁻¹ s⁻¹)³ is considerably more reactive than toluene ($k_{OH} = 0.6 \times 10^{-11}$ cm³ molecule⁻¹ s⁻¹)³ and 1,2-dihydroxybenzene ($k_{OH} = 10.4 \times 10^{-11}$ cm³ molecule⁻¹ s⁻¹)²² is 7 times more reactive than *o*-xylene ($k_{OH} = 1.4 \times 10^{-11}$ cm³ molecule⁻¹ s⁻¹).³ A similar pattern exists for the methyl-substituted phenols where the methylphenols and dimethylphenols are more reactive than the dimethylbenzenes and trimethylbenzenes, respectively.³ Finally, the fact that the OH rate coefficients for the dimethylphenols (2 CH₃ groups, 1 OH group) are lower than those for the 1,2-dihydroxymethylbenzenes (1 CH₃ group, 2 OH groups) also confirms the greater degree of ring activation conferred by the hydroxyl group.

The position of the OH and CH₃ substituents on the ring also appears to have a profound influence on the reactivity of the phenolic compounds. Both substituents donate electron density to the ortho and para positions and the compounds with the

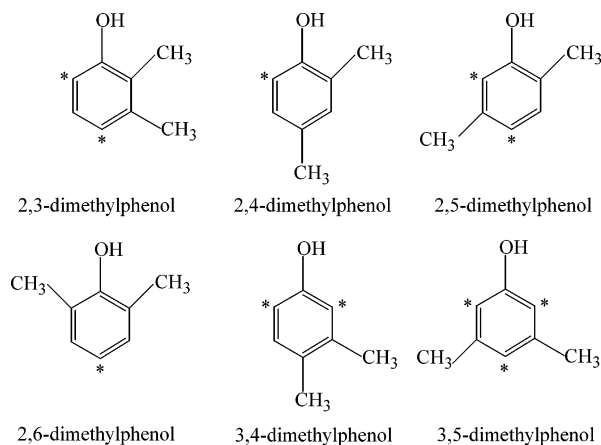


Figure 5. Six dimethylphenol isomers and the sites that are activated by the hydroxyl group toward electrophilic addition.

largest number of activated sites are thus the most reactive. Positions that are activated by OH groups are significantly more reactive than those activated by CH₃ groups. Although the OH group will activate all ortho and para positions, the presence of a CH₃ group at these sites provides steric hindrance to electrophilic addition and consequently leads to a reduction in the reactivity. The unoccupied sites activated by the OH groups in the dimethylphenol isomers are illustrated in Figure 5. 3,5-Dimethylphenol contains three sites activated by the hydroxyl group (the same three sites are also activated by the CH₃ group) and is the most reactive of the dimethylphenols toward OH radicals. 2,4- and 2,6-dimethylphenol only contain one site activated by the hydroxyl group and, as a result, are the least reactive of the dimethylphenol isomers. The remaining three isomers, 2,3-, 2,5-, and 3,4-dimethylphenol all contain two sites activated by the hydroxyl group and are correspondingly less reactive than 3,5-dimethylphenol but more reactive than 2,4- and 2,6-dimethylphenol.

The same argument can be used to explain the reactivity of the cresols, trimethylphenols, and 1,2-dihydroxymethylbenzene isomers toward OH radicals. In *o*- and *p*-cresol, the hydroxyl group activates two different sites on the ring, whereas in *m*-cresol, it activates three sites (the same three sites are also activated by the CH₃ group). As a result, *m*-cresol is the most reactive isomer; *o*- and *p*-cresol are less reactive than *m*-cresol and have similar rate coefficients.

The gas-phase reaction of NO₃ with phenolic compounds occurs through a different mechanism. Nitric acid (HNO₃) is produced and the overall reaction is thus equivalent to a H-atom abstraction process from the OH group. However, it is believed that the initial step in the reaction is NO₃ addition to the ring at the same position occupied by the OH group.¹³ This results in the formation of a six-membered transition state which subsequently eliminates HNO₃ and produces a phenoxy radical. The mechanism is used to explain the fact that phenol ($k_{\text{NO}_3} = 4.0 \times 10^{-12} \text{ cm}^3 \text{ molecule}^{-1} \text{ s}^{-1}$)³ is significantly more reactive toward NO₃ radicals than toluene ($k_{\text{NO}_3} = 7.0 \times 10^{-17} \text{ cm}^3 \text{ molecule}^{-1} \text{ s}^{-1}$).³ The very low reactivity of toluene and the xylenes with NO₃³ indicates that H-atom abstraction from the CH₃ substituents is very slow and therefore not important when the reactivity of the methyl-substituted phenols is considered.

As in the OH reactions, the reactivity of the phenolic compounds toward NO₃ radicals increases with the number of substituent hydroxyl or methyl groups. For example, the order of reactivity in the methyl-substituted phenols is dimethylphenol > methylphenol (cresol) > phenol. Similarly, the methyl-substituted 1,2-dihydroxybenzenes are more reactive than 1,2-

dihydroxybenzene, which in turn, is significantly more reactive than phenol. Because H-atom abstraction from the CH₃ groups is of negligible importance, then the observed increase in reactivity with the increasing number of CH₃ groups is due to the electron donating effect of the CH₃ groups. As discussed above, the CH₃ group donates electron density to the aromatic ring and activates the ortho and para positions toward electrophilic addition. Because the electrophilic NO₃ radical undergoes addition to the ring at the same position occupied by the OH group, then any methyl groups positioned ortho and para to the OH group will activate the site of addition, causing an increase in the reactivity. As shown in Table 2, *o*-cresol and 2,6-dimethylphenol are the most reactive of their respective isomers toward NO₃ radicals. Both compounds contain CH₃ groups in the ortho position(s) and are thus optimally activated toward NO₃ addition. *p*-Cresol and 2,4-dimethylphenol, with CH₃ groups in the para position(s), are also expected to show the same high level of reactivity. However, this is not the case and possibly indicates that the influence of CH₃ groups in the ortho positions are greater than those in the para position or that other substituent effects (e.g., affect on O–H bond strength) need to be considered. Nevertheless, the remaining compounds seem to fit the pattern; *m*-cresol and 3,5-dimethylphenol, with CH₃ groups in the meta position(s), are the least reactive of their respective isomers, and 2,3-, 2,5-, and 3,4-dimethylphenol, with one CH₃ group in the ortho or para position and the other in the meta position exhibit intermediate reactivity.

Atmospheric Implications. The gas-phase reactions of OH and NO₃ radicals with the dimethylphenols are fast and are thus expected to be the major atmospheric sinks for these compounds. The relative importance of OH and NO₃ for the removal of the dimethylphenols can be determined from calculations of the atmospheric lifetimes as shown in Table 1. The short atmospheric lifetimes for reaction with OH and NO₃ radicals indicate that both degradation processes are important. Reaction with OH radicals will dominate during daylight hours and reaction with NO₃ will be the major sink at night-time. The short atmospheric lifetimes also indicate that, if released into or formed in the atmosphere, the dimethylphenols will react rapidly and thus contribute to regional ozone formation. To determine their true impact, information on the reaction products and also the ability of these reactions to form secondary organic aerosol is needed. Such studies are currently in progress in our laboratory.

Acknowledgment. We thank Dr. Klaus Brockmann and the technical staff at the University of Wuppertal for their considerable help in the design and installation of the White Mirror system. This work was supported by Enterprise Ireland and the European Commission through the research project EXACT (EVK2-1999-00332) and the award of a Marie Curie Fellowship (EVK2-CT2000-50009) to L.P.T. We also acknowledge the support of the Environmental RTDI Program 2000-2006, financed by the Irish Government under the National Development Plan and administered on behalf of the Department of the Environment and Local Government by the Environmental Protection Agency.

References and Notes

- (1) Houweling, S.; Dentener, F.; Lelieveld, J. *J. Geophys. Res.* **1998**, *103*, 10673–10696.
- (2) Derwent, R. G.; Jenkin, M. E.; Saunders, S. M. *Atmos. Environ.* **1996**, *30*, 181–199.
- (3) *The Mechanisms of Atmospheric Oxidation of Aromatic Hydrocarbons*; Calvert, J. G., Atkinson, R., Becker, K. H., Kamens, R. M.,

Seinfeld, J. H., Wallington, T. J., Yarwood, G., Eds.; Oxford University Press, Oxford, 2002.

(4) Atkinson, R. *J. Phys. Chem. Ref. Data* **1994**, *2*, 47.

(5) Rinke, M.; Zetzsch, C. *Ber. Bunsen-Ges. Phys. Chem.* **1984**, *88*, 55–62.

(6) Knispel, R.; Koch, R.; Siese, M.; Zetzsch, C. *Ber. Bunsen-Ges. Phys. Chem.* **1990**, *94*, 1375–1379.

(7) Semadeni, M.; Stocker, D. W.; Kerr, J. A. *Int. J. Chem. Kinet.* **1995**, *27*, 287–304.

(8) Perry, R. A.; Atkinson, R.; Pitts, J. N., Jr. *J. Phys. Chem.* **1977**, *81*, 1607–1611.

(9) Atkinson, R.; Darnall, K. R.; Pitts, J. N., Jr. *J. Phys. Chem.* **1978**, *82*, 2759–2761.

(10) Atkinson, R.; Aschmann, S. M. *Int. J. Chem. Kinet.* **1990**, *22*, 59–67.

(11) Carter, W. P. L.; Winer, A. M.; Pitts, J. N., Jr. *Environ. Sci. Technol.* **1981**, *15*, 829–831.

(12) Atkinson, R.; Carter, W. P. L.; Plum, C. N.; Winer, A. M.; Pitts, J. N., Jr. *Int. J. Chem. Kinet.* **1984**, *16*, 887–898.

(13) Atkinson, R.; Aschmann, S. M.; Arey, J. *Environ. Sci. Technol.* **1992**, *26*, 1397–1403.

(14) Bolzacchini, E.; Bruschi, M.; Hjorth, J.; Meinardi, S.; Orlandi, M.; Rindone, B.; Rosenbohm, E. *Environ. Sci. Technol.* **2001**, *35*, 1791–1797.

(15) Rea, G. J. Ph.D. Thesis, University College Cork, 2004.

(16) Taylor, W. D.; Allston, T. D.; Moscato, M. J.; Fazekas, B. B.; Kozlowski, R.; Takacs, G. A. *Int. J. Chem. Kinet.* **1980**, *12*, 231–240.

(17) Kramp, F.; Paulson, S. E. *J. Phys. Chem. A* **1998**, *102*, 2685–2690.

(18) Prinn, R. G.; Weiss, R. F.; Miller, B. R.; Huang, F. N.; Alyea, J.; Cunnold, D. M.; Fraser, P. J.; Hartley, D. E.; Simmonds, P. J. *Science* **1995**, *269*, 187–192.

(19) Atkinson, R. *J. Phys. Chem. Ref. Data* **1991**, *84*, 437.

(20) Volkamer, R.; Platt, U.; Wirtz, K. In *The European Photoreactor (EUPHORE), 3rd Annual Report 2000*; Barnes, I., Sidebottom, H., Eds.; Bergische Universität: Wuppertal, 2001; pp 1–8.

(21) Tse, C. W.; Flagan, R. C.; Seinfeld, J. H. *Int. J. Chem. Kinet.* **1997**, *29*, 523–525.

(22) Olariu, R. I.; Barnes, I.; Becker, K. H.; Klotz, B. *Int. J. Chem. Kinet.* **2000**, *32*, 696–702.

(23) Olariu, R. I.; Bejan, I.; Barnes, I.; Klotz, B.; Becker, K. H.; Wirtz, K. *Int. J. Chem. Kinet.* **2004**, *36*, 577–583.

(24) Olariu, R. I.; Klotz, B.; Barnes, I.; Becker, K. H.; Mocanu, R. *Atmos. Environ.* **2002**, *36*, 3685–3697.